JACS
JOURNAL OF THE AMERICAN CHEMICAL SOCIETY
Communication
pubs.acs.org/JACS

Isolation and Characterization of a Tetramethyliron(III) Ferrate: An Intermediate in the Reduction Pathway of Ferric Salts with MeMgBr

Malik H. Al-Afyouni, Kathlyn L. Fillman, William W. Brennessel, and Michael L. Neidig*

Department of Chemistry, University of Rochester, Rochester, New York 14627, United States

Supporting Information

ABSTRACT: While iron-catalyzed Kumada cross-coupling reactions with simple iron salts have been known since the early 1970s, the nature of the *in situ*-formed iron species remains elusive. Herein, we report the synthesis of the homoleptic tetralkyliron(III) ferrate complex $[MgCl(THF)_5][FeMe_4]$ from the reaction of $FeCl_3$ with MeMgBr in THF. Upon warming, this distorted square-planar $S = {}^3/_2$ species converts to the $S = {}^1/_2$ species originally observed by Kochi and co-workers with concomitant formation of ethane, consistent with its intermediacy in the reduction pathway of $FeCl_3$ to generate the reduced iron species involved in catalysis.

Nearly half a century after the introduction of an iron-catalyzed C−C cross-coupling system in the 1970s by Kochi,[1] researchers have endeavored to harness the reactivity of inexpensive, nontoxic, and environmentally benign simple ferric salts and have demonstrated that iron can be a highly effective catalyst for a variety of cross-coupling reactions.[2] Functional group tolerance, short reaction times, stereoselectivity, and mild reaction conditions are among the triumphs in this field that have encouraged many chemists to consider the feasibility of developing iron-catalyzed cross-coupling systems to the level of palladium systems. However, limited mechanistic understanding has in most cases curtailed systematic improvements in iron-catalyzed cross-coupling systems.

Significant efforts to identify the active iron catalyst in the coupling of alkylmagnesium nucleophiles with alkenyl bromides were undertaken by Kochi and co-workers using electron paramagnetic resonance (EPR) spectroscopy.[1e,f] The observation of a broad $S = {}^1/_2$ signal upon addition of Grignard to ferric salts at low (ca. −40 °C) temperatures led to the proposal of an iron(I) active species. Due to the absence of cryogenic EPR studies (e.g., $T < 50$ K) or other spectroscopic studies capable of observing $S > {}^1/_2$ species, no intermediates along the reduction pathway to form the proposed iron(I) active species from iron(III) starting materials in the presence of organomagnesium reagents could be observed.[3] While Kochi's studies were highly suggestive of a reduced active species,[1e] it was not until the impressive report by Fürstner and co-workers of a homoleptic tetramethyliron(II) ferrate complex $[(Me_4Fe)(MeLi)][Li(OEt_2)]_2$ synthesized from reaction of MeLi with $FeCl_3$ or $FeCl_2$ in Et_2O that an active species *structure* could be envisioned (Scheme 1).[4,5] This complex exhibits a color change from red to yellow as well as reactivity toward activated electrophiles when dissolved in THF.[5] Though this complex provides an invaluable

Scheme 1

Kochi (1971)

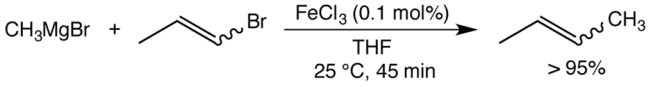

Fürstner (2006)

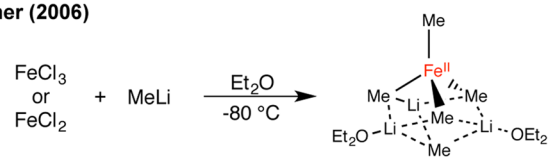

frame of reference, it should be noted that the color change upon dissolution in THF is highly suggestive of a structural change. While no reactivity toward electrophiles containing carbon−halide bonds was observed in diethyl ether in the initial work,[5] recent studies have shown that this iron(II)-ate species is active in both stoichiometric and catalytic ring-opening/cross-coupling reactions with MeMgBr.[6] However, an iron(II) center is not capable of generating the $S = {}^1/_2$ EPR signal observed by Kochi except in cases where the iron(II) center is part of a mixed-valence multinuclear system. Unfortunately, no methylated iron complexes isolated from *catalytically relevant* reagents for Kumada cross-coupling (i.e., THF solvent, methylmagnesium bromide) have been reported to date.

Herein we report the isolation and characterization of a homoleptic tetramethyliron(III) ferrate complex prepared from reaction of $FeCl_3$ and MeMgBr in THF—i.e., catalytically relevant iron salt, Grignard, and solvent. This complex is the first homoleptic methyl complex of iron(III), and it adopts a distorted square-planar geometry. Extensive EPR and density functional theory (DFT) studies show that this complex is an intermediate spin ($S = {}^3/_2$) system. Freeze-trapped *in situ* EPR spectroscopy directly tracks the conversion of this tetramethyliron(III) ferrate to the broad $S = {}^1/_2$ species previously observed by Kochi upon warming, with concomitant generation of ethane.

The addition of 4 equiv of methylmagnesium bromide to ferric chloride in THF at −80 °C results in a color change from green to orange. Despite the numerous difficulties in handling this highly air-, moisture-, and temperature-sensitive product, single orange crystals of **1** suitable for X-ray crystallography grown from a THF/hexane mixture at −80 °C reveal the iron-containing species to be $[MgCl(THF)_5][FeMe_4]\cdot THF$ (Figure 1). The solid-state structure of **1** is best described as a distorted square-

Received: August 6, 2014
Published: October 21, 2014

   dx.doi.org/10.1021/ja5080757 | J. Am. Chem. Soc. 2014, 136, 15457−15460

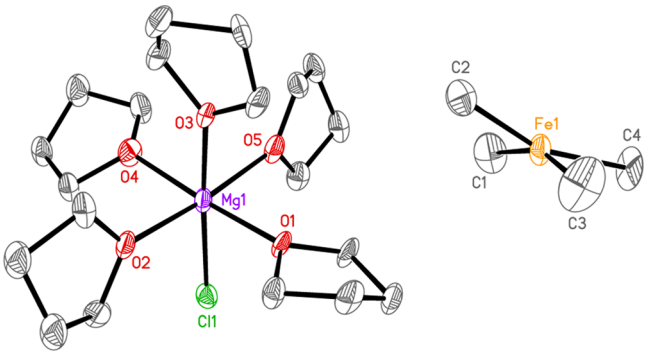

Figure 1. Crystal structure of **1**. Thermal ellipsoids are shown at 50% probability. H atoms and non-coordinated solvent are omitted for clarity. Selected bond lengths and angles: Fe1−C1 = 2.04(1) Å, Fe1−C2 = 2.05(1) Å, Fe1−C3 = 2.01(1) Å, Fe1−C4 = 2.05(1) Å, C1−Fe1−C2 = 94.7(7)°, C2−Fe1−C3 = 89.7(7)°, C3−Fe1−C4 = 91.1(7)°, C1−Fe1−C4 = 91.4(6)°, C1−Fe1−C3 = 158.7(7)°, C2−Fe1−C4 = 161.0(6)°. Note that the halide in the cation occurs in a ~0.4:0.6 ratio of Br:Cl in the crystal structure.

planar complex with a τ_4 parameter of 0.29.[7] The C−Fe−C angles in the plane are all close to 90° (ranging between 89.7° and 94.7°). Complex **1** is one of only a few reported compounds in the Cambridge Structural Database[8] that feature a methyl group bound to Fe(III).[5,9,10] The Fe−C bond lengths range between 2.01(1) and 2.05(1) Å and are consistent with the methyl Fe−C bond in the π-allyl complex $Cp^*Fe(C_3H_5)(CH_3)$ at 2.01 Å.[5] In contrast to its lithiated iron(II) analogue, $[(Me_4Fe)(MeLi)][Li(OEt_2)]_2$, the anionic ferric center in **1** displays no discernible interaction with the cation $MgCl(THF)_5$, indicating that coordinating solvents may play an important role in cation sequestration during catalysis. Since no other tetramethyl complexes of iron(III) exist in the literature, the most relevant comparison to **1** is the homoleptic tetrabenzyl-iron(III) complex $[MgCl(THF)_5][FeBn_4]$ synthesized by Bedford and co-workers, which adopts a tetrahedral geometry at iron(III) (τ_4 parameter of 0.97).[11] In contrast to thermally stable $[MgCl(THF)_5][FeBn_4]$, **1** is exceptionally temperature sensitive, undergoing rapid decomposition in the solid state above −40 °C. Gas is evolved from the crystalline solid during decomposition. Importantly, upon warming **1** to −40 °C in THF solution, a color change from orange to yellow slowly occurs.

The spin state of **1** is not immediately obvious due to its unusual geometry. In a previously reported ferric σ-organoiron complex, $[Li(THF)_4][Fe(C_6Cl_5)_4]$, an admixture of $S = {}^3/_2$ and $S = {}^5/_2$ spin states was observed in a distorted square-planar geometry leading to a complicated 10 K EPR spectrum.[12] To probe the electronic structure of **1**, low-temperature EPR spectroscopy was employed. The 10 K EPR spectrum of **1** in THF features an axial $S = {}^3/_2$ signal with $g \approx 4.20$ and 1.99 (Figure 2). Solution (THF) and solid samples of **1** give identical 10 K EPR spectra (see Supporting Information (SI), Figure S1), albeit with some line broadening in the solid sample due to intermolecular spin−spin relaxation, indicating that no significant structural change occurs in solution. Identical EPR spectra are also obtained from the reaction of $FeCl_3$ with excess MeMgBr (20 equiv) (see SI).

Encouraged by the interesting electronic properties of **1**, we probed the axial zero-field splitting (ZFS) parameter by temperature-dependent EPR spectroscopy (see SI for details). To obtain D, EPR spectra of **1** were collected between 4 and 40 K (SI, Figure S2). The normalized intensity data were fit to a Curie

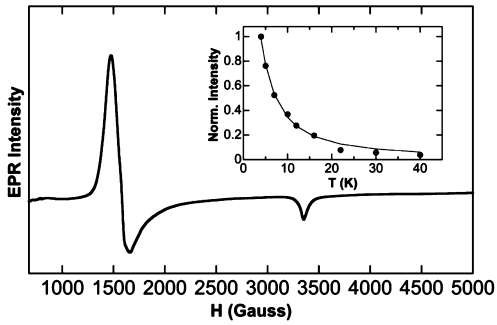

Figure 2. 10 K EPR spectrum of **1** in THF generated from reaction of $FeCl_3$ with MeMgBr. Inset shows the temperature-dependent EPR intensity of **1** and Boltzmann fit to the Curie law to give an axial ZFS parameter of $D = 6.5 \pm 0.5$ cm^{-1}.

law-dependent Boltzmann distribution as described in the SI to give $D = 6.5 \pm 0.5$ cm^{-1}. While known D values of $S = {}^3/_2$ iron(III) complexes are rare, it is noteworthy that this value of D is smaller than those previously reported for the antiferromagnetically coupled ($S = {}^3/_2$) high-spin iron(III)-NO species Fe-IPNS-ACV-NO as well as $Fe(L^{ISQ})_2Cl$ (D = 12.5 and 18 cm^{-1}, respectively).[13,14]

Spin-unrestricted DFT calculations of **1** were performed using the TZVP basis set on all atoms, including the $MgCl(THF)_5$ cation. The PBEPBE functional was employed in geometry optimizations for all possible spin states, and the calculated quartet structural parameters are in excellent agreement with the crystal structure (see SI). Additionally, single-point calculations on the optimized coordinates using the B3LYP functional predict that the calculated $S = {}^3/_2$ structure is the most energetically favorable, with the calculated $S = {}^1/_2$ structure 25 kcal/mol higher in energy, and the calculated $S = {}^5/_2$ structure 9 kcal/mol higher in energy. These calculations are consistent with the EPR spectroscopic results and the assignment of **1** as a $S = {}^3/_2$ system. The molecular orbital (MO) energy level diagram obtained from the calculated ground-state wave function of **1** is shown in Figure 3. The ground-state electronic structure can be described by the frontier MOs in the β-manifold, which show that the three lowest unoccupied MOs (β31, β32, and β33) and the highest occupied MO (β30) exhibit almost entirely Fe d-orbital character (>80%). MO β35 displays contributions from Fe (45%) and the four

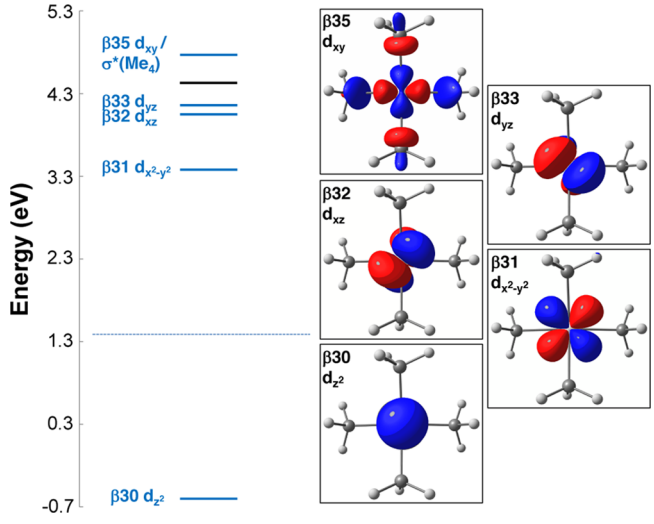

Figure 3. Calculated molecular orbital energy diagram for **1**.

dx.doi.org/10.1021/ja5080757 | J. Am. Chem. Soc. 2014, 136, 15457−15460

methyl groups (55% total). Interestingly, the $d_{x^2-y^2}$ orbital lies between the methyl groups and does not exhibit any bonding interactions. Alternatively, the d_{xy} orbital is aligned directly with the four methyl ligands and engages in the strongest Fe−CH_3 interaction. The strong σ-bonding interaction between the Fe d_{xy} orbital and the four methyl ligands is apparent from the corresponding σ^* MO, which is unoccupied in both the α- and β-manifolds.

It is interesting to consider the origin of the unusual distorted square-planar geometry (and $S = {}^3/_2$ ground state) of **1**. This geometry is particularly surprising considering that the tetrabenzyl complex, $[MgCl(THF)_5][FeBn_4]$ (denoted herein as $FeBn_4^-$), adopts a distorted tetrahedral geometry suggestive of a high-spin state as described by Bedford and co-workers.[11] To evaluate the source of this geometric preference, charge decomposition analysis was performed on optimized structures of both **1** and $FeBn_4^-$ (see SI for details). The analysis of quartet **1** and sextet $FeBn_4^-$ shows that the total net donation to iron from the ligands (sum of α and β contributions) is comparable in both systems (2.429 and 2.463 e^- for **1** and $FeBn_4^-$, respectively). Not surprisingly, the total net donation to the fully unoccupied iron(III) β-manifold in sextet $FeBn_4^-$ is significantly greater (by 0.957 e^-) than that of the fully occupied α-manifold. In contrast, the net donation to iron(III) in quartet **1** is more balanced between the α- and β-manifolds. When **1** is calculated as a sextet (tetrahedral geometry), the trend observed is similar to that in the sextet $FeBn_4^-$ (higher donation to β-manifold); however, the total donation (sum of α and β contributions) to iron(III) is less by 0.166 e^- when compared to quartet **1**. Thus, the adoption of a distorted square-planar geometry in **1** is necessary to maximize the donation of electron density to the iron(III) center by the four methyl ligands. It is interesting to note that, while the quartet of $FeBn_4^-$ would also maximize charge donation to iron(III) (see SI), the sextet is lowest in energy due to steric clashes of the benzyl ligands in the flattened tetrahedral quartet which disfavor this structure.

In order to evaluate the role of **1** in cross-coupling, both the potential reactivity of **1** toward electrophile and the possible formation of the reduced $S = {}^1/_2$ species at elevated temperature observed by Kochi were investigated.[1e,f] EPR studies of the reaction of **1** with excess 1-bromopropene at −80 °C showed no loss of the $S = {}^3/_2$ signal after 2 h of reaction (see SI), indicating no consumption of **1**. Combined with the poor thermal stability of **1** relative to the temperatures employed for cross-coupling, **1** is not an active catalytic species. Alternatively, **1** could represent an initial, transmetalated iron(III) species formed prior to reduction to the $S = {}^1/_2$ species observed by Kochi (where concomitant evolution of ethane was observed). To evaluate this hypothesis, EPR studies of the evolution of a solution of **1** generated at −80 °C upon warming were performed (Figure 4). While at −80 °C only the $S = {}^3/_2$ EPR signal corresponding to **1** is observed, warming toward −40 °C leads to the generation of a new $S = {}^1/_2$ species (where the sample is freeze-trapped after warming for the designated time). Elongated warming times result in a continued increase in the $S = {}^1/_2$ species, and warming to room temperature results in no remaining **1** in solution (i.e., complete loss of the $S = {}^3/_2$ signal) and only the $S = {}^1/_2$ species is observed. The $S = {}^1/_2$ spectrum and the corresponding yellow solution are identical to the previous observations of Kochi, indicating the formation of the same reduced species from the warming of **1** as Kochi found in reactions of $FeCl_3$ with excess MeMgBr in THF.[1e,f] While Kochi observed ethane evolution in the formation of the $S = {}^1/_2$ species,[1d−f] we observed ethane

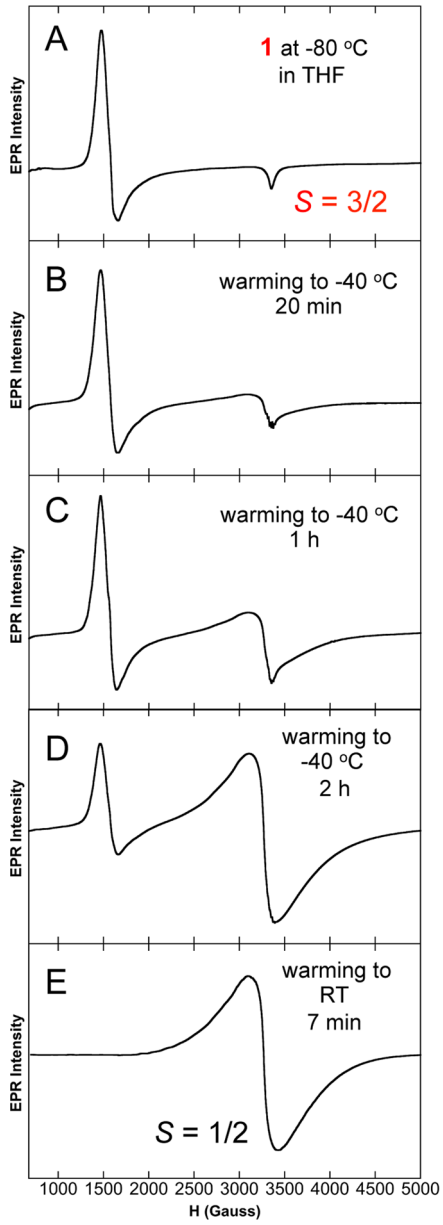

Figure 4. 10 K EPR spectra of the iron species in solution upon warming **1** in THF. (A) **1** in THF at −80 °C. (B−D) Warming **1** from −80 to −40 °C for (B) 20 min, (C) 1 h, and (D) 2 h. (E) Warming **1** from −80 °C to room temperature for 7 min. All samples were freeze-trapped in liquid nitrogen at the designated time points.

formation by GC/MS upon warming of **1**, consistent with the reduction of **1** to form the $S = {}^1/_2$ species through reductive elimination of ethane (see SI). Consistent with the intermediacy of **1** in the reduction pathway (Scheme 2), the reaction of $FeCl_3$ with MeMgBr at −40 °C (followed by freeze-trapping at 2 min)

Scheme 2

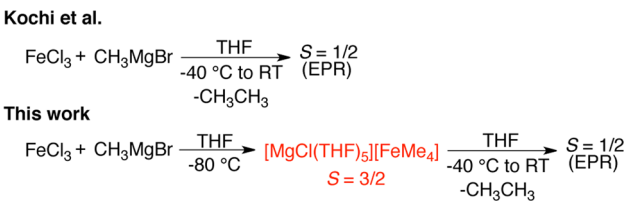

dx.doi.org/10.1021/ja5080757 | J. Am. Chem. Soc. 2014, 136, 15457−15460

results in an EPR spectrum analogous to that found upon warming **1** from −80 toward −40 °C. Finally, the $S = {}^1/_2$ species formed upon warming corresponds to effectively all of the iron in solution (95 ± 10% by EPR spin integration), demonstrating that all of **1** formed *in situ* is transformed to the $S = {}^1/_2$ species following reduction.

Once it was established that **1** is an intermediate in the reduction pathway of $FeCl_3$ with MeMgBr, it was interesting to consider whether reduction occurs directly from **1** or via a potentially multimetallic pathway. Using a 1:1 mixture of *in situ*-generated tetramethyliron(III) from independent reactions of $FeCl_3$ with CH_3MgBr and CD_3MgBr, respectively, formation of CD_3CH_3 was observed by GC/MS (see SI). This result would be consistent with a bimetallic or multimetallic reductive elimination pathway contributing to formation of the $S = {}^1/_2$ species. Such multimetallic species may form during initial reaction with Grignard and/or during reduction. The observation that *in situ*-formed **1** accounts for ∼50% of all iron in solution at −80 °C via EPR spin integration (see SI) further supports the formation of such multimetallic species which, in contrast to monomeric iron(III), can be EPR silent (i.e., integer spin or $S = 0$). However, possible contributions from multiple reduction pathways may exist. Future efforts to elucidate the structure of the $S = {}^1/_2$ species should provide further insight into the reduction pathway(s), including any potential involvement of additional methylated iron intermediates in forming the final $S = {}^1/_2$ species, proposed by Kochi to be the active species in catalysis.[1d]

Last, it is interesting to note the importance of cation and solvent effects in determining the iron species formed *in situ* in reactions of $FeCl_3$ with methyl Grignards. Whereas Fürstner previously demonstrated that reaction with MeLi in Et_2O leads to formation of a distorted tetrahedral tetramethyliron(II) ferrate,[4,5] herein we have shown that reaction with MeMgBr in THF alternatively generates a distorted square-planar tetramethyliron(III) ferrate. Thus, it is evident that the nature of the solvent (Et_2O vs THF) and cation (Li vs Mg) can result in the generation of significantly different iron species in solution. Furthermore, the nature of the halide can also affect iron speciation, as substitution of MeMgI for MeMgBr in THF leads to no EPR-active species being formed *in situ* at −80 °C or upon warming to room temperature (see SI). These significant differences in iron speciation as a function of solvent, cation, and halide can contribute to differences in catalytic activity for cross-coupling with methyl nucleophiles.

In summary, we have reported the synthesis and characterization of the homoleptic tetralkyliron(III) ferrate complex $[MgCl(THF)_5][FeMe_4]$ from the reaction of $FeCl_3$ with MeMgBr in THF—i.e., catalytically relevant Grignard and solvent. Importantly, *in situ* freeze-trapped EPR studies indicate that this novel $S = {}^3/_2$ species converts to the $S = {}^1/_2$ iron species proposed by Kochi to be active in cross-coupling with concomitant evolution of ethane, indicating that $[MgCl(THF)_5][FeMe_4]$ is an intermediate in the reduction pathway from $FeCl_3$. Further studies focusing on the direct synthesis and characterization of other iron-ate species formed in Kumada cross-coupling systems with simple iron salts, including the $S = {}^1/_2$ species, should continue to unravel the nature of the active iron species and the underlying mechanism of catalysis.

■ ASSOCIATED CONTENT

Supporting Information

Supplementary data and discussions of the experimental and theoretical methods. This material is available free of charge via the Internet at http://pubs.acs.org.

■ AUTHOR INFORMATION

Corresponding Author

neidig@chem.rochester.edu

Notes

The authors declare no competing financial interest.

■ ACKNOWLEDGMENTS

This work was supported by a grant from the National Institutes of Health (R01GM111480 to M.L.N.). The authors also acknowledge the Center for Integrated Research Computing at the University of Rochester for providing the necessary computing systems and support to enable the computational research presented in this study. We also thank Jared Kneebone for his assistance with figure production.

■ REFERENCES

(1) (a) Tamura, M.; Kochi, J. K. *J. Am. Chem. Soc.* **1971**, *93*, 1487. (b) Tamura, M.; Kochi, J. K. *J. Organomet. Chem.* **1971**, *31*, 289. (c) Tamura, M.; Kochi, J. K. *Bull. Chem. Soc. Jpn.* **1971**, *44*, 3063. (d) Neumann, S. M.; Kochi, J. K. *J. Org. Chem.* **1975**, *40*, 599. (e) Smith, R. S.; Kochi, J. K. *J. Org. Chem.* **1976**, *41*, 502. (f) Kwan, C. L.; Kochi, J. K. *J. Am. Chem. Soc.* **1976**, *98*, 4903.

(2) (a) Sherry, B. D.; Fürstner, A. *Acc. Chem. Res.* **2008**, *41*, 1500. (b) Fürstner, A.; Martin, R. *Chem. Lett.* **2005**, *34*, 624. (c) Bolm, C.; Legros, J.; Paih, J. L.; Zani, L. *Chem. Rev.* **2004**, *104*, 6217. (d) Czaplik, W. M.; Mayer, M.; Cvengros, J.; Wangelin, A. J. v. *ChemSusChem* **2009**, *2*, 396. (e) Jana, R.; Pathak, T. P.; Sigman, M. S. *Chem. Rev.* **2011**, *111*, 1417. (f) Cahiez, G.; Avedissian, H. *Synthesis* **1998**, 1199. (g) Fürstner, A.; Leitner, A.; Mendez, M.; Krause, H. *J. Am. Chem. Soc.* **2002**, *124*, 13856. (h) Nakamura, M.; Matsuo, K.; Ito, S.; Nakamura, E. *J. Am. Chem. Soc.* **2004**, *126*, 3686. (i) Kuzmina, O. M.; Steib, A. K.; Flubacher, D.; Knochel, P. *Org. Lett.* **2012**, *14*, 4818. (j) Bedford, R. B.; Betham, M.; Bruce, D. W.; Danopoulos, A. A.; Frost, R. M.; Hird, M. *J. Org. Chem.* **2006**, *71*, 1104. (k) Bedford, R. B.; Brenner, P. B.; Carter, E.; Carvell, T. W.; Cogswell, P. M.; Gallagher, T.; Harvey, J. N.; Murphy, D. M.; Neeve, E. C.; Nunn, J.; Pye, D. R. *Chem.—Eur. J.* **2014**, *20*, 7935.

(3) Berthold, H. J.; Spiegl, H. J. *Z. Anorg. Allg. Chem.* **1972**, *391*, 193.

(4) Fürstner, A.; Krause, H.; Lehmann, C. W. *Angew. Chem., Int. Ed.* **2005**, *45*, 440.

(5) Fürstner, A.; Martin, R.; Krause, H.; Seidel, G.; Goddard, R.; Lehmann, C. W. *J. Am. Chem. Soc.* **2008**, *130*, 8773.

(6) Sun, C.-L.; Fürstner, A. *Angew. Chem., Int. Ed.* **2013**, *52*, 13071.

(7) Yang, L.; Powell, D. R.; Houser, R. P. *Dalton Trans.* **2007**, 955.

(8) Allen, F. H. *Acta Crystallogr.* **2002**, *B58*, 380.

(9) Dawkins, G. M.; Green, M.; Orpen, A. G.; Stone, F. G. A. *J. Chem. Soc., Chem. Commun.* **1982**, 41.

(10) Tilset, M.; Fjeldahl, I.; Hamon, J.-R.; Hamon, P.; Toupet, L.; Saillard, J.-Y.; Costuas, K.; Haynes, A. *J. Am. Chem. Soc.* **2001**, *123*, 9984.

(11) Bedford, R. B.; Brenner, P. B.; Carter, E.; Cogswell, P. M.; Haddow, M. F.; Harvey, J. N.; Murphy, D. M.; Nunn, J.; Woodall, C. H. *Angew. Chem., Int. Ed.* **2014**, *53*, 1804.

(12) Alonso, P. J.; Arauzo, A. B.; Fornies, J.; Garcia-Monforte, M. A.; Martin, A.; Martinez, J. I.; Menjon, B.; Rillo, C.; Saiz-Garitaonandia, J. J. *Angew. Chem., Int. Ed.* **2006**, *45*, 6707.

(13) Brown, C. D.; Neidig, M. L.; Neibergall, M. B.; Lipscomb, J. D.; Solomon, E. I. *J. Am. Chem. Soc.* **2007**, *129*, 7427.

(14) Chun, H.; Bill, E.; Weyhermuller, T.; Wieghardt, K. *Inorg. Chem.* **2003**, *42*, 5612.